Removal of boron from aqueous solution using cryptocrystalline magnesite

Vhahangwele Masindi and Mugera W. Gitari

ABSTRACT

The present study aimed to evaluate the efficiency of using cryptocrystalline magnesite to remove boron ions from aqueous systems. Batch experimental protocols were used to evaluate the adsorption capacity of magnesite for boron. Parameters optimized included: time, dosage, chemical species concentration and pH. Optimum conditions were observed to be 30 min of agitation, 1 g dosage of magnesite per 100 mL of aqueous solution and 20 mg/L initial boron concentration. Removal of boron from aqueous solution was observed to be independent of initial pH of the aqueous solution. The adsorption of boron onto magnesite was observed to fit better to pseudo-second-order kinetics than pseudo-first-order kinetics hence proving chemisorption. The intra-particle diffusion model revealed that the adsorption of boron from aqueous system occurs through multiple reaction phenomena. Adsorption isotherms proved that the removal of boron by magnesite fitted well to both Langmuir and Freundlich adsorption isotherms hence proving that both mono- and multi-site adsorption processes are taking place. Under optimized conditions, magnesite was able to attenuate the boron concentration to <0.01 mg/L which is below levels stipulated in World Health Organization guidelines. It was concluded that this comparative study will be helpful for further application of magnesite in remediation of boron-contaminated aqueous systems.

Key words | adsorption, boron ions, cryptocrystalline magnesite, isotherms, kinetics

Vhahangwele Masindi (corresponding author)
CSIR (Council for Scientific and Industrial Research), Built Environment,
Hydraulic Infrastructure Engineering (HIE),
PO Box 395,
Pretoria 0001,
South Africa
E-mail: *vmasindi@csir.co.za*; *masindivhahangwele@gmail.com*

Mugera W. Gitari
Environmental Remediation and Pollution Chemistry Research Group, Department of Ecology and Resources Management, School of Environmental Science,
University of Venda,
P/bag X5050,
Thohoyandou 0950,
South Africa

INTRODUCTION

Pollution of water by boron has caused serious environmental problems that require intensive environmental mitigation (Masindi *et al.* 2016a). Boron can enter the environment through natural processes and anthropogenic activities. Naturally, boron is found in association with coal and gold seams, and other mineral seams. After mining, it is exposed to weathering, hence boron leaches to surface and underground water resources. Anthropogenically, it enters the environment through the use of fertilizers, insecticides, corrosion inhibitors, antifreeze, cooling systems, pharmaceuticals, dyes, bleaching agents, detergents and nuclear reactors (Türker *et al.* 2014). These industrial uses generate boron-rich wastewaters that are discharged to aquatic ecosystems. In aqueous environments, boron exists as boric acid [$B(OH)_3$] in acidic conditions and borate [$B(OH)_4^-$] in basic conditions (Türker *et al.* 2014).

Boron plays a significant role in plant and animal growth. It inhibits prostaglandins and leukotriene, which are mediators in inflammatory conditions; stimulates production of oestrogen in menopausal woman; reduces the severity of inflammatory conditions associated with rheumatoid arthritis; may inhibit the incidence of prostate

doi: 10.2166/wrd.2016.012

cancer; may help prevent post-menopausal osteoporosis; and inhibits enzymatic function to produce anti-inflammatory effects (Hilal *et al.* 2011; Wang *et al.* 2014). However, it has very narrow nutritional significance and if present above a threshold level, it becomes a socio-economic and environmental problem. On agricultural soils, it forms complexes with toxic heavy metals (e.g. Cu, Cd, Ni, Pb), thus posing hazardous effects to plant and other organisms (Hilal *et al.* 2011; Türker *et al.* 2014). For safe intake, the World Health Organization recommended 0.3 mg/L concentration of boron in water for domestic use (Masindi 2013; Masindi *et al.* 2016b). For plants and irrigation purposes, safe exposure concentration is 0.3 mg/L for sensitive plants, 1–2 mg/L for semi-sensitive plants and 2–4 mg/L for tolerant plant species (Masindi *et al.* 2016b).

Thus, water containing elevated concentrations of boron need to be contained and treated to prevent contamination of surface and groundwater (Fujita *et al.* 2005; del Mar de la Fuente García-Soto & Camacho 2006; Dydo & Turek 2013). A number of methods have been developed for boron removal, including precipitation (Irawan *et al.* 2011), reverse osmosis (Cengeloglu *et al.* 2008; Kabay *et al.* 2010; Hilal *et al.* 2011), adsorption (Kıpçak & Özdemir 2012; Polowczyk *et al.* 2013), ion exchange (Kabay *et al.* 2006; Hilal *et al.* 2011; Dydo & Turek 2013), filtration (Dydo *et al.* 2005), desalination, phytoremediation (Türker *et al.* 2013) and selective resins (Hilal *et al.* 2011; Santander *et al.* 2013).

Natural and unprocessed raw materials are potential low cost adsorbents for decontamination of wastewaters (Masindi *et al.* 2015a). Calcined crystalline magnesite, calcite and dolomite have been used with good effect for boron removal (Kıpçak & Özdemir 2012; Masindi *et al.* 2016a). Amorphous (cryptocrystalline) magnesite alone has never been used for boron removal (Masindi *et al.* 2016a). The primary aim of this study was to evaluate the potential of cryptocrystalline magnesite for use in boron removal. It has been estimated that the cryptocrystalline magnesite mine in Folovhodwe, Limpopo Province, South Africa (22°35′47.0″S and 30°25′33″E) has deposits of close to 20 MT which can be mined for the coming 20 years (Masindi *et al.* 2015c). Thus, the use of cryptocrystalline magnesite is expected to be an economically viable way of removing boron from wastewater.

MATERIALS AND METHODS

Sampling of the adsorbent

Raw magnesite rocks were collected before any processing at the mine from the Folovhodwe Magnesite Mine. Magnesite samples were milled to a fine powder using a Retsch RS 200 miller (Haan, The Netherlands) and passed through a 32-μm particle size sieve. After sieving, the samples were tightly kept in zip lock plastic bags until use.

Preparation of standard working solutions

A stock solution containing 500 mg/L of boron ions was prepared by using analytical grade H_3BO_3 (Lab Consumables Supply, South Africa). Working solutions with different concentrations were prepared using appropriate dilutions of stock solution.

Characterization

Boron concentration was determined using inductively coupled plasma mass spectrometry (ICP-MS) (7500ce, Agilent, Alpharetta, GA, USA). The mineralogical composition of magnesite was ascertained using X-ray diffraction. Morphology and elemental composition were determined using scanning electron microscopy coupled with electron dispersion spectrometry (SEM–EDS) (JOEL, JSM–840, Hitachi, Tokyo, Japan). Surface area was measured by the Brunauer-Emmett-Teller (BET) method (Tristar II 3020, Micromeritics BET, Norcross, GA, USA).

Batch experiments: optimization of boron adsorption conditions

Optimization experiments were done in batch experimental procedures. Parameters optimized include contact time, magnesite dosage, initial boron concentration and pH. A table shaker was used for all the experiments (1300E, Labcon, Petaluma, CA, USA). All experiments were done in triplicate and the results were reported as mean values.

Effect of shaking time

To evaluate the effect of equilibration time on the removal of boron, shaking time was varied from 1 to 360 min. Fixed parameters were: initial boron concentration 10 mg/L; magnesite in aqueous solution 1 g/100 mL; initial pH <6; 250 rpm shaking; and room temperature.

Effect of magnesite dosage

To evaluate the effect of magnesite dosage, the dosage was varied from 0.1 to 8 g. Fixed parameters were boron 10 mg/L; reaction time 30 min; initial pH <6; 250 rpm shaking; and room temperature.

Effect of chemical species concentration

To evaluate the effect of initial boron concentration, the initial concentrations were varied from 0.1 to 60 mg/L. Fixed parameters were 1 g magnesite per 100 mL of solution; reaction time 30 min; initial pH <6; 250 rpm shaking; and room temperature.

Effect of pH

To evaluate the effect of initial pH, the initial pH was varied from 2 to 12. The initial pH was adjusted by using 0.1 M of NaOH and nitric acid. Fixed parameters were boron 10 mg/L; reaction time 30 min; 1 g magnesite per 100 mL of solution; 250 rpm shaking; and room temperature.

Optimized conditions obtained from the batch experiments were used in experiments to treat boron rich wastewater.

Calculation of boron removal and adsorption capacity

Computation of % removal and adsorption capacity was done using Equations (1) and (2).

$$\text{Percentage removal (\%)} = \left(\frac{C_i - C_e}{C_i}\right) \times 100 \quad (1)$$

$$\text{Adsorption capacity } (q_e) = \frac{(C_i - C_e)V}{m} \quad (2)$$

where: C_i = initial concentration, C_e = equilibrium ion concentration, V = volume of solution and m = mass of magnesite.

Adsorption kinetics

Adsorption kinetics was done using pseudo-first-order kinetic, pseudo-second-order kinetic and intra-particle diffusion models (Masindi *et al.* 2015b).

Adsorption isotherms

Adsorption isotherms were determined using Langmuir and Freundlich adsorption models (Masindi *et al.* 2015b).

RESULTS AND DISCUSSION

Mineralogical composition by X-ray diffraction

The mineralogical composition of cryptocrystalline magnesite is presented in Figure 1.

The results revealed that cryptocrystalline magnesite consists of magnesite, dolomite, periclase, brucite, forsterite and quartz as the main constituents. The wide broadening of X-ray diffraction patterns and some sharp peaks indicates that the material is cryptocrystalline in nature. This corroborates SEM–EDS results and a study by Nasedkin *et al.* (2001).

Scanning electron microscopy–elemental dispersive spectrometry analysis

The spot elemental composition and morphology of magnesite is shown in Figure 2.

The SEM image indicates that magnesite is composed mostly of aggregates with particle sizes generally below 1 μm. The elemental content of magnesite was determined using EDS at four spots. The analysis showed that the mineral is composed of Mg, C and O with weight percentage (wt %) of 43.9, 9.4 and 44.4, respectively. The impurities Si and Ca were also observed on cryptocrystalline magnesite surfaces. Again, the results correspond to arithmetic averages of four data points obtained from randomly selected locations on the surface of magnesite hence validating the EDS on each point.

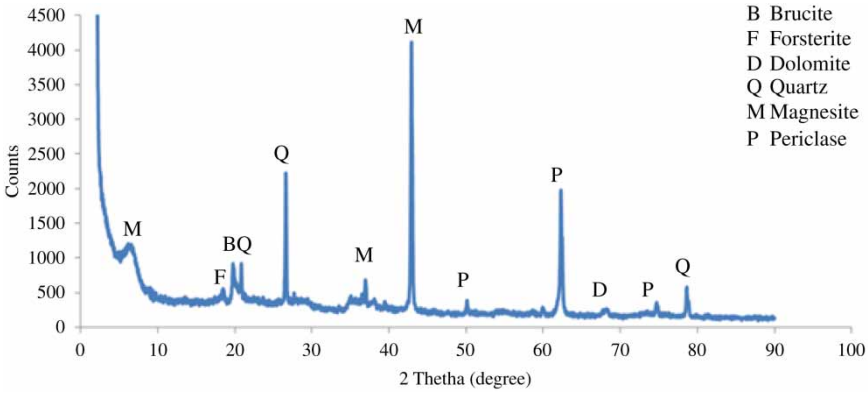

Figure 1 | Mineralogical composition of cryptocrystalline magnesite.

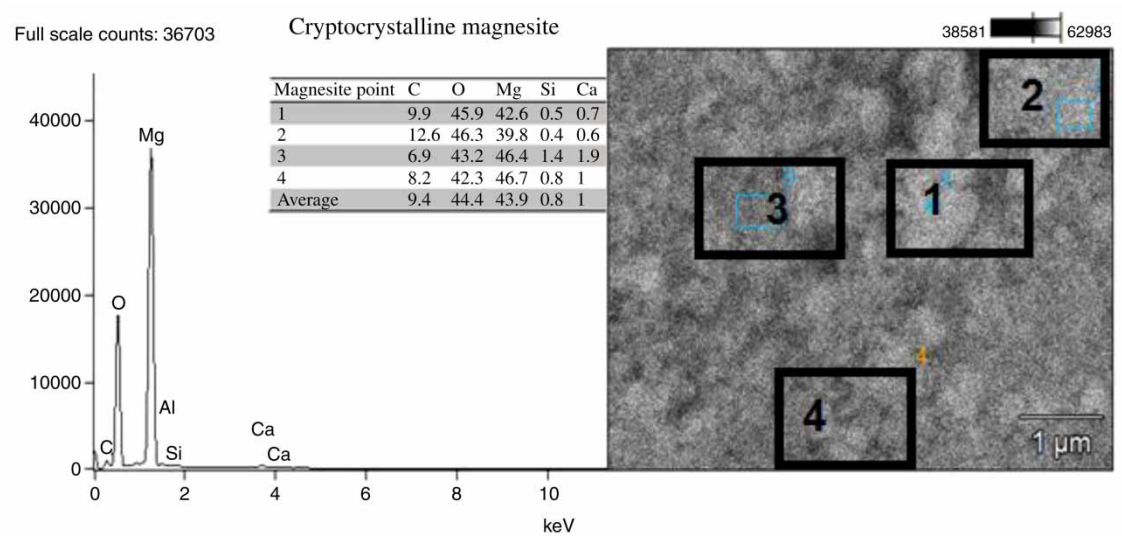

Figure 2 | Spot elemental composition and morphology of cryptocrystalline magnesite.

Surface area by BET

The surface area of South African magnesite from Folovhodwe is shown in Table 1.

Table 1 | Surface area of Folovhodwe magnesite

Parameter	Magnesite
BET surface area (m^2/g)	14.6
Micropore area (cm^3/g)	2.3
External surface area (m^2/g)	12.3
Micropore volume (m^2/g)	0.0009
Adsorption average pore diameter (4V/A by BET) (m^2/g)	223

BET revealed that magnesite has a surface area of 14.6 m^2/g, which is the sum of micropore area and external surface area. It has mean pore diameter of 223 Å. The large pore diameter of magnesite allows boron ions to diffuse into the pore channel of the mesoporous material due to smaller radius of boron species. Therefore, boron can be adsorbed onto the surfaces of magnesite through outer and inner sphere complexes.

Optimization experiments

Optimum boron removal conditions by cryptocrystalline magnesite were established by evaluating the effects of

agitation time, magnesite dosage, initial boron concentration and initial pH.

Figure 3(a) shows the effect of contact time on removal of boron: the adsorption of boron increases with increase in contact time. From the first minute of interaction, the uptake of boron was strong. This may be attributed to many surfaces being available for sorption of boron by magnesite. After 30 min, there was no further significant removal of boron ions observed hence, indicating that the adsorbent is saturated with boron or boron has been depleted from the aqueous system. From these results, it was concluded that the optimum equilibration time for the subsequent experiment is 30 min. Cryptocrystalline magnesite showed rapid boron removal abilities as compared to calcined magnesite (420 min) (Kıpçak & Özdemir 2012) and magnesium oxide (30 min) (del Mar de la Fuente García-Soto & Camacho 2006). Figure 3(b) shows the effect of various dosages on removal of boron from aqueous solution was evaluated. According to Kıpçak & Özdemir (2012), as the dosage increases, more surfaces which are suitable for adsorption are present and vacant. As shown in Figure 3(b), as the dosage increases, there was an increase in boron removal:

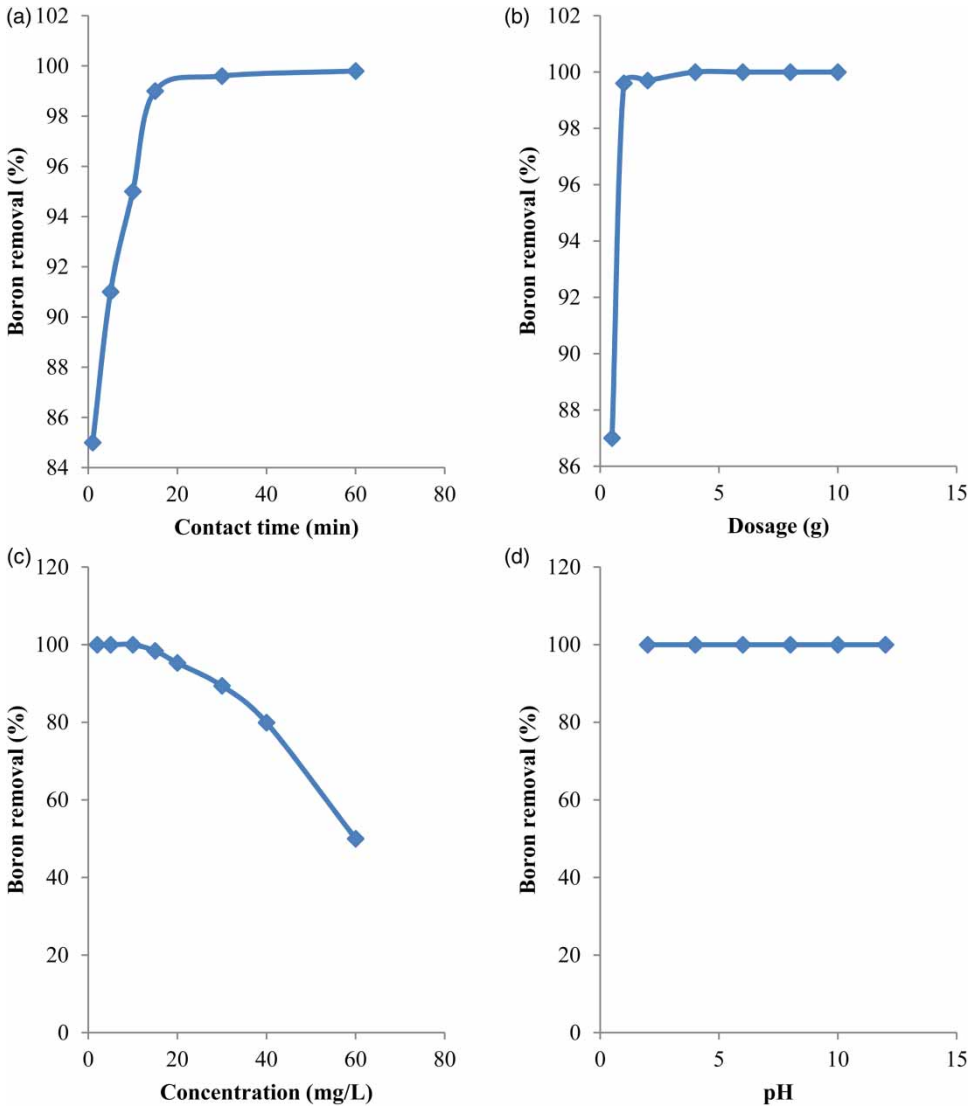

Figure 3 | Effect of contact time, magnesite dosage, initial boron concentration and initial pH on percentage removal of boron.

from 0.5 g/100 mL to 1 g/100 mL, the adsorption of boron by magnesite was very rapid and above 1 g/100 mL no more notable change was observed denoting that the adsorption has reached equilibrium. The flattening of the adsorption curve above 1 g/100 mL shows that boron has been depleted from the aqueous system. As such, 1 g/100 mL was taken as the optimum dosage for the subsequent experiments. Figure 3(c) shows the percentage removal of boron decreases with an increase in initial boron concentration. This is attributed to more ions being introduced to aqueous system hence saturating the vacant sites on the surface of the adsorbent. At low concentration, more site for adsorption are available than ions and at high concentration, more ions are available than adsorption sites. From 0.1 to 20 mg/L the adsorption of boron was rapid and above 20 mg/L, the adsorption capacity decreased gradually hence indicating that the adsorbent was saturated with boron. However, 20 mg/L has been chosen as the optimum concentration for the subsequent experiments. Figure 3(d) shows the percentage removal of boron with varying pH. The initial pH was in the range 2 to 12. Variation of boron concentration with varying supernatant pH showed that the removal of boron by magnesite is independent of initial pH level. Dissolution of magnesite leads to an increase in pH of the solution to pH >10. At alkaline pH, boron exists as an oxyanion. Oxyanionic boron will be adsorbed to Mg^{2+} cations in solution or co-precipitate with $Mg(OH)_2$. Similar results were obtained by Kıpçak & Özdemir (2012) when using magnesite tailings.

Modelling of experimental results

Adsorption kinetics

The effect of contact time on removal of boron from aqueous solution was evaluated using different kinetic models to reveal the nature of the adsorption process and rate-limiting processes. A Lagergren pseudo-first-order kinetic model is a well-known model that is used to describe mechanisms of species adsorption by an adsorbent. It can be written as follows (Masindi *et al.* 2015b):

$$\ln (q_e - q_t) = \ln q_e - k_1 t \quad (3)$$

where k_1 (min^{-1}) is the pseudo-first-order adsorption rate coefficient and q_e and q_t are the values of the amount adsorbed per unit mass at equilibrium and at time t, respectively. The experimental data were fitted by using the pseudo-first-order kinetic model by plotting $\ln(q_e - q_t)$ vs t, and the results are shown in Table 2. The pseudo-first-order was applied and it was found to converge poorly with the experimental data; the correlation coefficient was <0.95. Moreover, the calculated amounts of boron ions adsorbed by magnesite [q_e, calc (mg g^{-1})] were less than the experimental values [$q_{e,\ exp}$ (mg g^{-1})] (Table 2). The finding indicated that the Lagergren pseudo-first-order kinetic model is inappropriate to describe the adsorption of boron ions from aqueous system by magnesite.

The pseudo-second-order kinetic model is another kinetic model that is widely used to describe the adsorption process from an aqueous solution. The linearized form of the pseudo-second-order rate equation is given as follows:

$$\frac{t}{qr} = \frac{1}{k_2 q_e^2} + \frac{t}{q_e} \quad (4)$$

where k_2 [g (mg min^{-1})] is the pseudo-second-order adsorption rate constant and q_e and q_t are the values of the amount adsorbed per unit mass at equilibrium and at time t, respectively. An application of the pseudo-second-order rate equation for adsorption of chemical species to magnesite showed a better fit with experimental data (Table 2). The results obtained confirm that pseudo-second-order model is the more suitable kinetic model to describe adsorption of boron ions by magnesite from aqueous systems. Moreover, this also confirms that the mechanism of boron removal from aqueous solution is chemisorption. Different

Table 2 | Different kinetic model parameters for adsorption of boron on magnesite

Adsorption kinetics			
R^2	$Q_{e(exp)}$	$Q_{e\ (cal)}$	
Pseudo-first-order kinetic			
0.95	1	11.1	0.4
Pseudo-second-order kinetic			
1	1	1	1.9
Intra-particle-diffusion model			
0.7	1	0.85	0.07

kinetic model parameters for adsorption of boron ions are shown in Table 2. Note the theoretical adsorption capacity is close to the experimental adsorption capacity further confirming that this model describes the adsorption data. The overall kinetics of the adsorption from solutions may be governed by the diffusional processes as well as by the kinetics of the surface chemical reaction as proposed by Weber and Morris (Masindi *et al.* 2015b). To determine whether film diffusion or intra-particle diffusion is the rate limiting step, the intra-particle diffusion model parameters were calculated (Table 2). The model suggested that if the sorption mechanisms are via intraparticle diffusion then a plot of q_t vs $t^{1/2}$ will be linear and intraparticle diffusion is the only rate limiting step when such plot passes through the origin. When the sorption process is controlled by more than one mechanism, then the plot of q_t vs $t^{1/2}$ will be multi-linear. Intra-particle diffusion is computed using the following expression:

$$q_t = k_{\mathrm{id}} t^{1/2} + C_i \tag{5}$$

where k_{id} (mg g^{-1} $min^{-1/2}$) is the intra-particle diffusion coefficient (slope of the plot of q_t vs $t^{1/2}$) and C_i is the intra-particle diffusion rate constant.

The C value (Table 2) indicate the thickness of the boundary layer which was observed to be very small for magnesite thus suggesting that surface diffusion plays a lesser role as the rate-limiting step in the overall sorption process.

Adsorption isotherms

The relationship between the amounts of ions adsorbed and the ion concentration remaining in solution is described by an isotherm. The two most common isotherm models for describing this type of system are the Langmuir and Freundlich adsorption isotherms (Masindi *et al.* 2015b). These models describe adsorption processes on a homogenous (monolayer) or heterogeneous (multilayer) surface, respectively. The most important model of monolayer adsorption came from Langmuir (Masindi *et al.* 2015b). This isotherm is given as:

$$q_e = \frac{Q_0 b C_e}{1 + bC_e} \tag{6}$$

The constants Q_0 and b are characteristics of the Langmuir equation and can be determined from a linearized form of Equation (6). The Langmuir isotherm is valid for monolayer adsorption onto a surface with a finite number of identical sites and can be expressed in the following linear form:

$$\frac{C_e}{Q_e} = \frac{1}{Q_m b} + \frac{C_e}{Q_m} \tag{7}$$

where, C_e = equilibrium concentration (mg/L), Q_e = amount adsorbed at equilibrium (mg/g), Q_m = Langmuir constant related to adsorption capacity (mg/g) and b = Langmuir constant related to energy of adsorption (L/mg).

A plot of C_e/Q_e vs C_e should be linear if the data conform to the Langmuir isotherm. The value of Q_m is determined from the slope and the intercept of the plot. It is used to derive the maximum adsorption capacity and b is determined from the original equation and represents the degree of adsorption.

The Freundlich adsorption isotherm describes the heterogeneous surface energy by multilayer adsorption and is expressed as:

$$q_e = kC_e^{1/n} \tag{8}$$

The equation may be linearized by taking the logarithm of both sides of the equation and can be expressed in linear form as:

$$\log q_e = \frac{1}{n} \log C_e + \log K \tag{9}$$

where C_e = equilibrium concentration (mg/L), q_e = amount adsorbed at equilibrium (mg g^{-1}), K_f = partition coefficient (mg/g) and n = degree of adsorption.

A linear plot of log q_e vs log C_e indicates whether the data conform to the Freundlich isotherm. The value of K_f implies that the energy of adsorption on a homogeneous surface is independent of surface coverage and n is an adsorption constant which reveals the rate at which adsorption takes place. These two constants are determined from the slope and intercept of the plot of each isotherm. The results from isotherm modelling suggest that both Freundlich ($R^2 = 0.95$) and Langmuir ($R^2 = 0.94$) models fit better

to the adsorption of boron onto magnesite matrices. This result demonstrates that the adsorption process was taking place on both homogeneous and heterogeneous surface. Q_{max} and b were determined from the slope and intercept of the plot and were found to be 5.4 and 27.64, respectively. Q_m was similar to experimental Q_e, thus confirming the better fit. K_f and n were calculated from the slopes of the Freundlich plots. The constants were found to be $K_f =$ 199,526.2 and 0.5, respectively. The n values between 1 and 10 represent beneficial adsorption. This show adsorption of ions from aqueous solution by magnesite was favourable. The parameters of Langmuir and Freundlich adsorption isotherms are shown in Table 3.

Table 3 | Parameters of Langmuir and Freundlich adsorption isotherms

Adsorption isotherms			
Langmuir adsorption isotherm			
R^2	b (L/mg)	Q_m (mg/g)	$Q_{e(exp)}$
0.95	27.64	5.4	6
Freundlich adsorption isotherm			
R^2	n	K_f	$Q_{e(exp)}$
0.94	0.5	199,526.2	6

Comparison of adsorption capacities of materials used for removal of boron

A comparative study of different adsorbents for boron in contaminated water is shown in Table 4. Cryptocrystalline magnesite offers better adsorption capacity for boron as compared to other adsorbents except calcined magnesite. This suggests that cryptocrystalline magnesite can also be used as an alternative technology in place of conventional methods for treatment of boron. Moreover, other treatment methods require pre-treatment of the adsorbent which is costly. The present study uses raw magnesite which is not pre-treated.

Table 4 | Comparison of adsorption capacities of materials used for removal of boron

Adsorbents	Adsorption capacity (mg/g)	Reference
Cryptocrystalline magnesite	6	Present study
Magnesite/bentonite composite	4	Masindi *et al.* (2016a)
Goethite	0.3	Goli *et al.* (2011)
Calcined magnesite	57	Kıpçak & Özdemir (2012)
Siral 5	1	Yurdakoç *et al.* (2005)
Siral 40	1	Yurdakoç *et al.* (2005)
Siral 80	1	Yurdakoç *et al.* (2005)
Camlica bentonite 1 (CB2)	3	Öztürk & Kavak (2008)
Camlica bentonite 2 (CB2)	0.1	Öztürk & Kavak (2008)

CONCLUSION

In this study, the feasibility of using cryptocrystalline magnesite as an alternative adsorbent for removal of boron from aqueous solution was evaluated. Batch experiments revealed that the optimum conditions for removal of boron from aqueous solution using cryptocrystalline magnesite is 30 min of shaking, 1 g of magnesite per 100 mL of aqueous solution and 20 mg L^{-1} initial boron concentration. The removal of boron was observed to be independent of initial pH of the solution. Under optimized conditions, cryptocrystalline magnesite managed to reduce boron concentration to below levels specified in WHO water quality guidelines. The adsorption of boron onto magnesite was observed to fit better to pseudo-second-order kinetic than pseudo-first-order-kinetic hence proving chemisorption. The intra-particle diffusion model revealed that the adsorption of boron from aqueous system is through multiple reaction phenomena. Adsorption isotherms proved that the removal of boron by magnesite fitted well to both Langmuir and Freundlich adsorption isotherm hence proving that both mono- and multisite adsorption are taking place. This study proved that cryptocrystalline magnesite can be used as low-cost material for removal of boron from contaminated water bodies.

ACKNOWLEDGEMENTS

The authors wish to convey their sincere gratitude to the Council of Scientific and Industrial Research (CSIR),

Research and Innovation Directorate, Department of Ecology and Resource Management, School of Environmental Sciences, University of Venda, SASOL-INZALO, National Research Foundation (NRF) and Department of Science and Technology (DST) (DST/NRF) for funding this project.

REFERENCES

Cengeloglu, Y., Arslan, G., Tor, A., Kocak, I. & Dursun, N. 2008 Removal of boron from water by using reverse osmosis. *Separation and Purification Technology* **64**, 141–146.

Del Mar De La Fuente García-Soto, M. & Camacho, E. M. 2006 Boron removal by means of adsorption with magnesium oxide. *Separation and Purification Technology* **48**, 36–44.

Dydo, P. & Turek, M. 2013 Boron transport and removal using ion-exchange membranes: a critical review. *Desalination* **310**, 2–8.

Dydo, P., Turek, M., Ciba, J., Trojanowska, J. & Kluczka, J. 2005 Boron removal from landfill leachate by means of nanofiltration and reverse osmosis. *Desalination* **185**, 131–137.

Fujita, Y., Hata, T., Nakamaru, M., Iyo, T., Yoshino, T. & Shimamura, T. 2005 A study of boron adsorption onto activated sludge. *Bioresource Technology* **96**, 1350–1356.

Goli, E., Rahnemaie, R., Hiemstra, T. & Malakouti, M. J. 2011 The interaction of boron with goethite: experiments and CD–MUSIC modeling. *Chemosphere* **82**, 1475–1481.

Hilal, N., Kim, G. J. & Somerfield, C. 2011 Boron removal from saline water: a comprehensive review. *Desalination* **273**, 23–35.

Irawan, C., Kuo, Y.-L. & Liu, J. C. 2011 Treatment of boron-containing optoelectronic wastewater by precipitation process. *Desalination* **280**, 146–151.

Kabay, N., Yilmaz, İ., Bryjak, M. & Yüksel, M. 2006 Removal of boron from aqueous solutions by a hybrid ion exchange–membrane process. *Desalination* **198**, 158–165.

Kabay, N., Güler, E. & Bryjak, M. 2010 Boron in seawater and methods for its separation – a review. *Desalination* **261**, 212–217.

Kıpçak, İ. & Özdemir, M. 2012 Removal of boron from aqueous solution using calcined magnesite tailing. *Chemical Engineering Journal* **189–190**, 68–74.

Masindi, V. 2013 Adsorption of Oxyanions of As, B, Cr, Mo and Se from Coal Fly Ash Leachates Using Al^{3+}/Fe^{3+} Modified Bentonite Clay. Masters Thesis, University of Venda.

Masindi, V., Gitari, M. W., Tutu, H. & De Beer, M. 2015a Passive remediation of acid mine drainage using cryptocrystalline magnesite: a batch experimental and geochemical modelling approach. *Water SA* **41**, 677–682.

Masindi, V., Gitari, M. W., Tutu, H. & Debeer, M. 2015b Efficiency of ball milled South African bentonite clay for remediation of acid mine drainage. *Journal of Water Process Engineering* **8**, 227–240.

Masindi, V., Gitari, W. M. & Ngulube, T. 2015c Kinetics and equilibrium studies for removal of fluoride from underground water using cryptocrystalline magnesite. *Journal of Water Reuse and Desalination* **5**, 282–292.

Masindi, V., Gitari, M. W., Tutu, H. & Debeer, M. 2016a Removal of boron from aqueous solution using magnesite and bentonite clay composite. *Desalination and Water Treatment* **57**, 8754–8764.

Masindi, V., Gitari, M. W. & Tutu, H. 2016b Adsorption of As, B, Cr, Mo and Se from coal Fly ash leachate by Fe^{3+} modified bentonite clay. *Journal of Water Reuse and Desalination* **6** (3), 382–391. doi: 10.2166/wrd.2015.207.

Nasedkin, V. V., Krupenin, M. T., Safonov, Y. G., Boeva, N. M., Efremova, S. V. & Shevelev, A. I. 2001 The comparison of amorphous (cryptocrystalline) and crystalline magnesites. *Mineralia Slovaca* **33**, 567–574.

Öztürk, N. & Kavak, D. 2008 Boron removal from aqueous solutions by batch adsorption onto cerium oxide using full factorial design. *Desalination* **223**, 106–112.

Polowczyk, I., Ulatowska, J., Koźlecki, T., Bastrzyk, A. & Sawiński, W. 2013 Studies on removal of boron from aqueous solution by Fly ash agglomerates. *Desalination* **310**, 93–101.

Santander, P., Rivas, B. L., Urbano, B. F., Yılmaz İpek, İ., Özkula, G., Arda, M., Yüksel, M., Bryjak, M., Kozlecki, T. & Kabay, N. 2013 Removal of boron from geothermal water by a novel boron selective resin. *Desalination* **310**, 102–108.

Türker, O. C., Böcük, H. & Yakar, A. 2013 The phytoremediation ability of a polyculture constructed wetland to treat boron from mine effluent. *Journal of Hazardous Materials* **252–253**, 132–141.

Türker, O. C., Vymazal, J. & Türe, C. 2014 Constructed wetlands for boron removal: a review. *Ecological Engineering* **64**, 350–359.

Wang, B., Guo, X. & Bai, P. 2014 Removal technology of boron dissolved in aqueous solutions – a review. *Colloid Surface A* **444**, 338–344.

Yurdakoç, M., Seki, Y., Karahan, S. & Yurdakoç, K. 2005 Kinetic and thermodynamic studies of boron removal by Siral 5, Siral 40, and Siral 80. *Journal of Colloid and Interface Science* **286**, 440–446.

First received 5 January 2016; accepted in revised form 8 April 2016. Available online 14 May 2016